

# Nanoscale

Accepted Manuscript



This is an *Accepted Manuscript*, which has been through the Royal Society of Chemistry peer review process and has been accepted for publication.

*Accepted Manuscripts* are published online shortly after acceptance, before technical editing, formatting and proof reading. Using this free service, authors can make their results available to the community, in citable form, before we publish the edited article. We will replace this *Accepted Manuscript* with the edited and formatted *Advance Article* as soon as it is available.

You can find more information about *Accepted Manuscripts* in the [Information for Authors](#).

Please note that technical editing may introduce minor changes to the text and/or graphics, which may alter content. The journal's standard [Terms & Conditions](#) and the [Ethical guidelines](#) still apply. In no event shall the Royal Society of Chemistry be held responsible for any errors or omissions in this *Accepted Manuscript* or any consequences arising from the use of any information it contains.

# Reactivity, Swelling and Aggregation of Mixed-Size Silicate Nanoplatelets

M. Segad,<sup>\*,†</sup> B. Cabane,<sup>‡</sup> and Bo Jönsson<sup>¶</sup>

*Advanced Light Source, Lawrence Berkeley National Laboratory, Berkeley, California 94720, United States, ESPCI, 10 Rue Vauquelin, 75231 Paris Cedex 5, France, and Theoretical Chemistry, Chemical Center, Lund University, POB 124, S-22100 Lund, Sweden*

E-mail: MSegadMeehdi@lbl.gov;M.Segad@gmail.com

## Abstract

Montmorillonite is a key ingredient in a number of technical applications. However, little is known regarding the microstructure and the forces between silicate platelets. The size of montmorillonite platelets from different natural sources can vary significantly. This has an influence on their swelling behavior in water as well as in salt solutions, particularly when tactoid formation occurs, that is when divalent counterions are present in the system. A tactoid consists of a limited number of platelets aggregated in a parallel arrangement with a constant separation. The tactoid size increases with platelet size and with very small nanoplatelets,  $\sim 30$  nm, no tactoids are observed irrespectively of the platelet origin and concentration of divalent ions. The formation and dissociation of tactoids seem to be reversible processes. A large proportion of small nanoplatelets

---

\*To whom correspondence should be addressed

<sup>†</sup>Advanced Light Source

<sup>‡</sup>ESPCI

<sup>¶</sup>Lund University

in a mixed-size system affects the tactoid formation, reduces the aggregation number and increases the extra-lamellar swelling in the system.

Keywords: SAXS, Osmotic stress, 3D-DLS, Fractal microstructure, Nanoplatelets.

## Introduction

An important phenomenon in any dispersion of platelets is the aggregation of platelets into so-called tactoid, that occurs with di- or trivalent counterions.<sup>1</sup> Several experimental studies have shown that an individual tactoid only consists of a dozen or so well-oriented platelets.<sup>2-5</sup> Blackmore and Miller<sup>6</sup> measured the silicate layer separations of Ca montmorillonite as a function of pressure by X-ray diffraction technique. Their results showed only small variations of the number of platelets per tactoid,  $N$ . Purely theoretical work of negatively charged lamellae<sup>7-9</sup> and platelet-like particles<sup>10</sup> have demonstrated that ion-ion correlations is a likely origin of tactoid formation. Experimental and Monte Carlo (MC) simulations results are in quantitative agreement for the distance between the platelets in a tactoid.<sup>11-13</sup> It is well established that aggregation in clay-water system leads to changes in swelling properties<sup>14</sup> as well as hydraulic conductivity.<sup>15</sup> For example, Martin and co-workers observed a significant increase of the hydraulic conductivity of Laponite platelets upon adding enough electrolytes.<sup>16</sup> This is an important observation for applications, where the clay is supposed to form a barrier, *e.g.* in waste barriers and geological storage technologies.

We have recently studied Ca and Na montmorillonites in pure water as well as in aqueous salt solutions through cryogenic transmission electron microscopy (cryo-TEM), small-angle X-ray scattering (SAXS)<sup>17-19</sup> and by osmotic swelling.<sup>20</sup> These studies have shown that there exist two types of lamellar swelling in Ca montmorillonite dispersions (*i.e.* intra- and extra-lamellar). In agreement with earlier studies, we have also found a limited number of platelets per tactoid in Ca montmorillonite, see Fig. 1. In addition, larger platelets give rise to larger tactoids, whereas for really small platelets no tactoid formation is observed.<sup>18</sup>

The latter observations offers a step toward understanding the tactoid formation and the swelling phenomenon in Ca montmorillonite with pure water and in the presence of 2:1 salt. A puzzling result, however, has been the significant extra-lamellar swelling displayed, where both SAXS studies and simulations predict the formation of tactoids with a very small swelling. Na montmorillonite, on the other hand, has a very strong swelling capacity in pure water or at low salt concentrations in agreement with theoretical predictions.

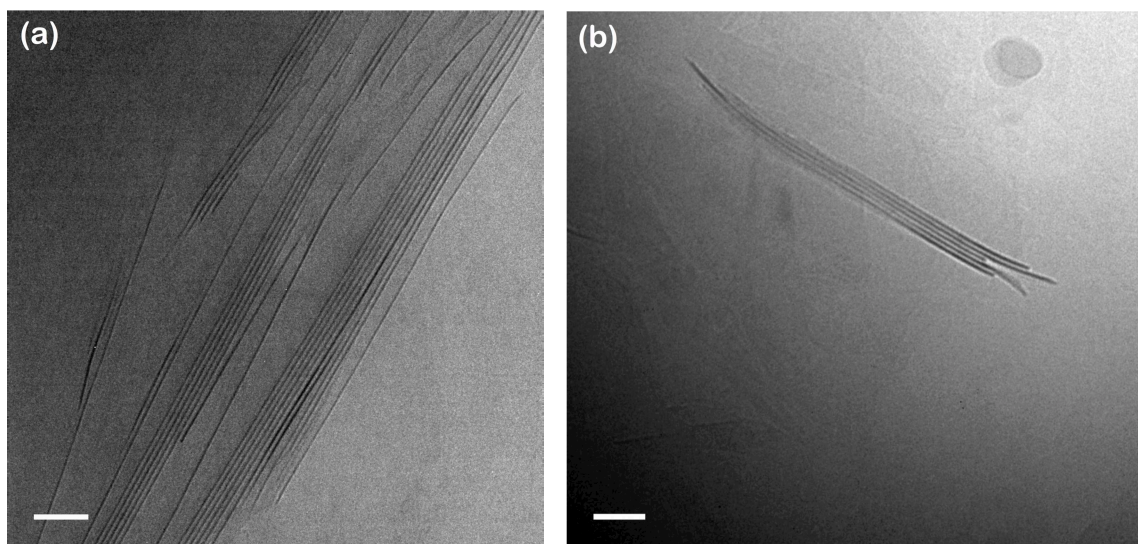


Fig. 1: (a) Cryo-TEM image of tactoid in calcium montmorillonite dispersion. (b) Note that smaller nanoplatelets form a smaller tactoid. The bars in the lower left corners correspond to 20 nm.<sup>17</sup>

As is mostly the case in natural or synthetic clays, the platelets are polydisperse in size and shape; hence it is difficult to establish whether the tactoids consist of mixed platelet sizes, or if there is a preference for certain platelet sizes in a tactoid. In this work, we have investigated the swelling, aggregation and dissociation of fractionated and unfractionated montmorillonite platelets from a number of silicate clays, in order to understand the effect of platelet size on structure and swelling. SAXS and three-dimensional dynamic light scattering (DLS) techniques were applied to provide information about the size as well as the microstructure of nanoplatelets in equilibrium with a bulk solution with given ionic composition and neutral pH.

## Experimental Section

### Materials purification

Three different bentonites as well as kaolin clay were used in this study. The sources of natural clays were Wyoming bentonite (MX80), Bavarian bentonite (Ba), Slovakian bentonite (Sk) and kaolin from Iraq. Further details of the characterization and the quantitative mineralogical compositions of Bavarian and Slovakian bentonites have been described by Kaufhold and Dohrmann.<sup>22,23</sup> Analytical grade sodium chloride (purity, 99.5%) was purchased from Merck and millipore water was used to prepare the solutions. Calcium chloride (purity, 98%) was purchased from Aldrich. SnakeSkin Dialysis Tubing (3.5 K MWCO, 1 ml) was bought from Pierce.

The first homoionic Na montmorillonite was obtained from MX80 after a careful purifying process. The procedure was as follows: 20 g of MX80 was dispersed in 2 L of millipore water and allowed to stand until the large particles,  $\geq 2 \mu\text{m}$ , had sedimented and various impurities were discarded. In order to reduce the amount of the multivalent ions, this suspension was washed by addition of 1 M NaCl solution three times: each time, the clay suspension was mixed with the aqueous salt solution and the mixture was left to equilibrate for at least a week. Then the clay suspension was washed three times with millipore water. In order to remove excess electrolytes, the Na montmorillonite (NaMX80) was transferred to dialysis membranes and placed into plastic containers with millipore water. The water was changed daily until the conductivity was below  $10 \mu\text{S}/\text{cm}$ . The raw Bavarian and Slovakian bentonites were treated in an identical purification process. The final stock suspensions of Na montmorillonites (NaMX80, NaBa and NaSk) were fractionated and then used as dispersions. The weight fractions of the samples were determined by drying the dispersions at 333 K.

Calcium montmorillonite (CaMX80) was prepared through similar purification process as described above. In this case unfractionated NaMX80 suspension ( $\sim 150 \text{ ml}$ ) was taken

and dispersed in 1 L of 1 M  $\text{CaCl}_2$ . The clay particles were left to settle, and a homogenous sediment was formed. The whole sediment was recovered and the procedure was repeated three times. In order to remove excess electrolytes, we also used the dialysis procedure. The final fractions were dried at 333 K. Unfractionated CaMX80 was used as a dry powder in the dialysis swelling experiment.

Chemical analysis was performed for kaolin and Wyoming clays by inductive coupled plasma-atomic emission spectrometry technique (ICP-AES), while the Bavarian and Slovakian bentonites was studied by X-ray fluorescence spectroscopy (XRF).<sup>22,23</sup> Loss of ignition was determined gravimetrically by ignition to  $\sim 1273$  K for 15 minutes. The cation exchange capacity (CEC) for Raw Ba, Raw Sk and MX80 are 67, 60 and 77 (meq/100 g), respectively. Table 1 summarizes the chemical composition of the clays.

Table 1: Chemical analysis of various clays.

Composition in wt-%	Raw Ba	Raw Sk	Kaolin	NaMX80	CaMX80	MX80
$\text{SiO}_2$	51.5	61.7	53.7	68	68	67
$\text{Al}_2\text{O}_3$	20.1	17.5	36.27	21	21	20
$\text{Fe}_2\text{O}_3$	5.9	8.1	1.8	4.0	3.9	3.9
MgO	2.9	1.6	0.43	2.2	2.1	2.2
CaO	1.4	1.3	0.2	0.1	2.4	1.2
$\text{Na}_2\text{O}$	0.1	0.4	0.71	3.8	0.3	2.7
$\text{K}_2\text{O}$	1.7	1.4	1.5	0.6	0.5	1.2
$\text{TiO}_2$	0.4	0.8	1.29	0.1	0.1	0.12
LOI	15.5	6.7	4.1	0.2	1.7	1.68

## Fractionation and sample preparation

A pure NaMX80 dispersion was centrifuged at 1500 rpm for 60 min, as a first step. The sediment from this still contains a range of particle sizes, therefore the material was re-dispersed in millipore water and centrifuged repeatedly to separate out the largest platelets. The collected sediment from the successive processes is the the coarse fraction. The medium and fine fractions of Na montmorillonite were obtained by repeating the same procedure

several times at higher speeds. The collected supernatant, from the first step, was centrifuged at 6000 rpm and then at 17000 rpm to obtain the medium and the fine fractions, respectively. As a result, NaMX80 dispersions were fractionated into three samples (NaMX80-I, NaMX80-II and NaMX80-III). Also, two fractions of NaBa (NaBa-I and NaBa-II) and two discrete fractions of NaSk (NaSk-I and NaSk-II) were obtained by the same protocol. Preparation of the sample was as follows: the SnakeSkin dialysis tubing was cut to appropriate lengths and put into millipore water for 24 h. One end of the dialysis tubing was folded over twice and attached. 10 g of either a dispersion comprising individual fraction (coarse, medium or fine) or a mixture of two clay fractions with different weight ratio were added, and the tubing was rolled up at the open end, pressed slightly to remove the air inside the pocket and then folded over twice and attached. The tubing was placed into 500 ml of 0.5 mM  $\text{CaCl}_2$  aqueous solution or millipore water in a shaking incubator hood system (from Bühler Germany) for up to a month.

### Small Angle X-ray Scattering (SAXS)

The small angle X-ray scattering (SAXS) experiments were performed at the synchrotron radiation facility MAX II in Lund using beamline I911-4.<sup>24,25</sup> A monochromatic beam of 0.91 Å wavelength was used together with point collimation and a two-dimensional, low noise and fast read-out pixel detector (PILATUS 1M). The sample to detector distance was 1.9 m ( $q = 0.1 - 3.9 \text{ nm}^{-1}$ ) with 2 min of exposure time. The SAXS data were analyzed with the program FIT2D.<sup>26</sup>

Clay samples were taken from dialysis experiments and measured in 1 mm quartz capillaries. The background scattering of pure water and salt concentrations were subtracted. The number of montmorillonite platelets per tactoid,  $N$ , that is tactoid size can be estimated from the scattering peaks by applying the Scherrer formula.<sup>21</sup> A model with an assumption of a Lorentzian line shape has been approximated to the scattering function based on that formula as follows:

$$q^2 I(q) \propto \frac{w}{(q - q_{max})^2 + w^2} \quad (1)$$

where  $I(q)$  is the scattering intensity and  $w$  a measure of the width. The width at half maximum of the peak is equal to  $2w$  and the average number of platelets per tactoid can be expressed as  $N = q_{max}/w$ .<sup>19</sup>

## Size determination

Three-dimensional dynamic light scattering (3D-DLS) instrument was used for simultaneous dynamic and static light scattering with transparent and turbid samples at a wavelength of 632 nm. The temperature of the sample was controlled by a circulating water bath at 298 K. The scattered light was detected within an angular range of 50–120° by two Avalanche Photo Diodes and processed by a Flex correlator in a three-dimensional cross-correlation configuration. Recent studies, which combined an imaging tool and DLS technique, demonstrated that the effective diameter,  $D_{eff}$ , of montmorillonite platelets from DLS correlates with the diameter obtained from cryo-TEM<sup>17,19</sup> and AFM<sup>27,28</sup> images. Here, DLS measurements were performed using a modulated 3D cross-correlation technique. This approach is justified by the fact that clay-water is a highly turbid system; hence, the use of this device with sufficient modulation speed suppresses multiple scattering and isolates the single scattering dynamic structure factor, which lead to more accurate determination of the size distribution than would have been possible by conventional DLS. In order to suppress multiple scattering further, very low clay volume fraction of each sample was filled into cylindrical glass cells of a diameter of 5 mm to shorten the scattered light path.<sup>29</sup>



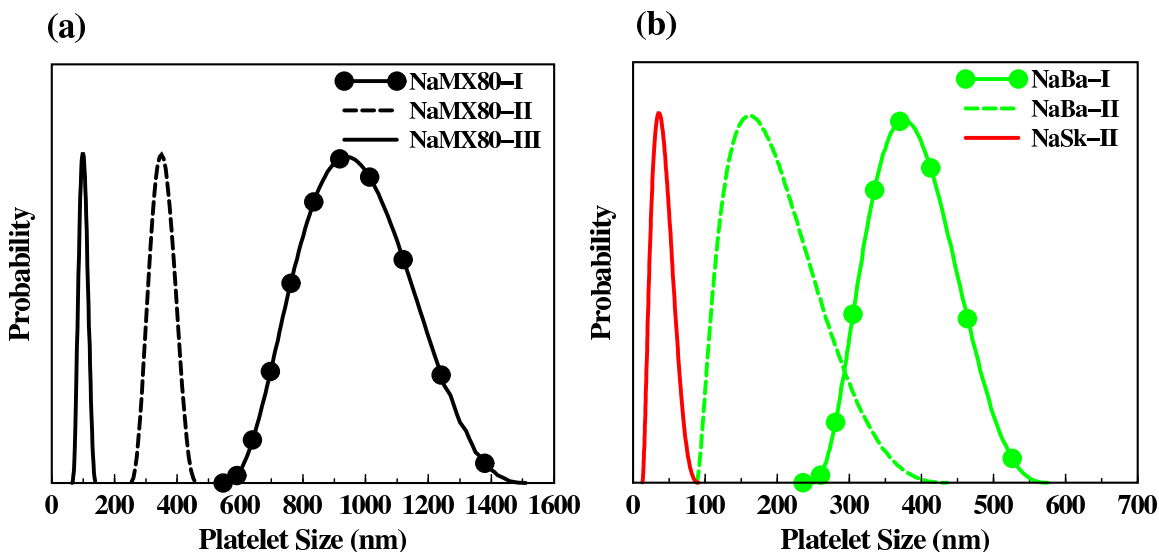


Fig. 2: Platelet size distribution, obtained through DLS measurements. (a) Solid line represents fraction III of NaMX80, dashed line comes from fraction II and solid line with circles is from fraction I. (b) Red solid line is from NaSk fraction II, green dashed line is from NaBa-II and green line with circles is from NaBa-I.

Table 2: Platelet size (nm),  $D_{eff}$ , in different clay fractions.

Fraction	NaMX80	NaBa	NaSk	kaolin
I	950	350	225 <sup>a</sup>	750
II	350	160	35	-
III	100	-	-	-

Approximate relative amount of each sample: For NaMX80-I (50%), NaMX80-II (40%) and NaMX80-III (< 10%). For NaBa-I (60%) and NaBa-II (< 40%). For NaSk-I (< 70%) and NaSk-II (30%). <sup>a</sup> Not used in this work.

## Results and discussion

### Determination of the platelet size distribution

Six homoionic Na montmorillonites were obtained from raw Wyoming MX80, Bavarian (Ba) and Slovakian (Sk) bentonites, respectively, through a purification and fractionation procedures. The different clays were fractionated by the same centrifugation protocol. The fractions are denoted as MX80-I, MX80-II, MX80-III, NaBa-I, NaBa-II and NaSk-II. Platelet size distribution for different clay fractions were extracted from DLS measurements. Fig. 2 shows the size distributions obtained from the various clay fractions. The platelet size distributions obtained after fractionation are quite different and also rather well separated. The

*effective* platelet diameters,  $D_{eff}$ , for NaBa, NaSk and NaMX80 fractions are summarized in Table 2. The Wyoming bentonite MX80-I is dominated by large platelets, whereas the two Bavarian and Slovakian clays consist of significantly smaller platelets.

### The origin of extra-lamellar swelling in Ca montmorillonite

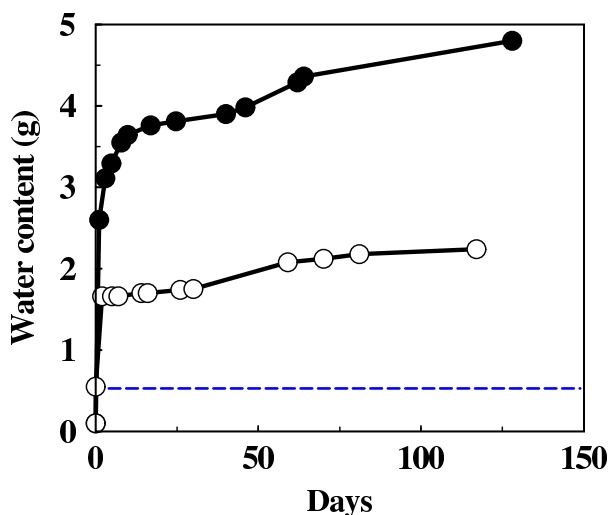


Fig. 3: Swelling of fractionated and unfractionated Ca montmorillonites. Dry powder (1 g) of CaMX80 obtained by ion exchange from fraction I of NaMX80 (open circles) and from unfractionated CaMX80 (filled circles) were placed in dialysis pockets and immersed in millipore water. The blue dashed line indicates the intra-lamellar swelling.

The swelling of fractionated and unfractionated CaMX80 clays have been monitored through the weight of the dialysis pockets over time. One gram of Ca clay was placed in a pocket made from a semipermeable membrane and immersed in millipore water. The water was changed at regular intervals, and the weights are plotted in Fig. 3. The clay dispersions in the dialysis pockets were allowed to equilibrate for up to four months. During that time, fractionated CaMX80-I as well as unfractionated CaMX80 swelled continuously.

As can be seen in Fig. 3, there is a fast initial swelling, taking place within a few hours, which goes beyond the intra-lamellar swelling, that is the formation of an approximately 1 nm thick water layer between the platelets. After this initial period, the extra-lamellar swelling continues with roughly the same long-term rates for both CaMX80-I and CaMX80. CaMX80-I containing only the largest platelets ( $\sim 950$  nm) swell much less than unfractionated

CaMX80. The latter contains different sizes, including medium and small platelets.<sup>18</sup> Smaller platelets mean weaker ion–ion correlation and thinner tactoids. The extra-lamellar swelling is correlated with the number of free platelets, which for Ca montmorillonite increases with decreasing platelet size. This result reveals the reason behind the discrepancy between the experimental data and theoretical prediction of swelling pressures for Ca montmorillonite, using molecular dynamics model.<sup>30</sup>

## Tactoid formation in size-fractionated platelets

Here we describe the formation of tactoids of three size-fractionated dispersions (*i.e.* NaMX80-I, NaMX80-II and NaMX80-III) in the presence of  $\text{Ca}^{2+}$  cations. The initial suspension for all three was an aqueous dispersion of Na montmorillonite. 10 g of each fraction were placed in a dialysis pocket and immersed in 0.5 L of 0.5 M  $\text{CaCl}_2$  and allowed to equilibrate at 298 K for a month.

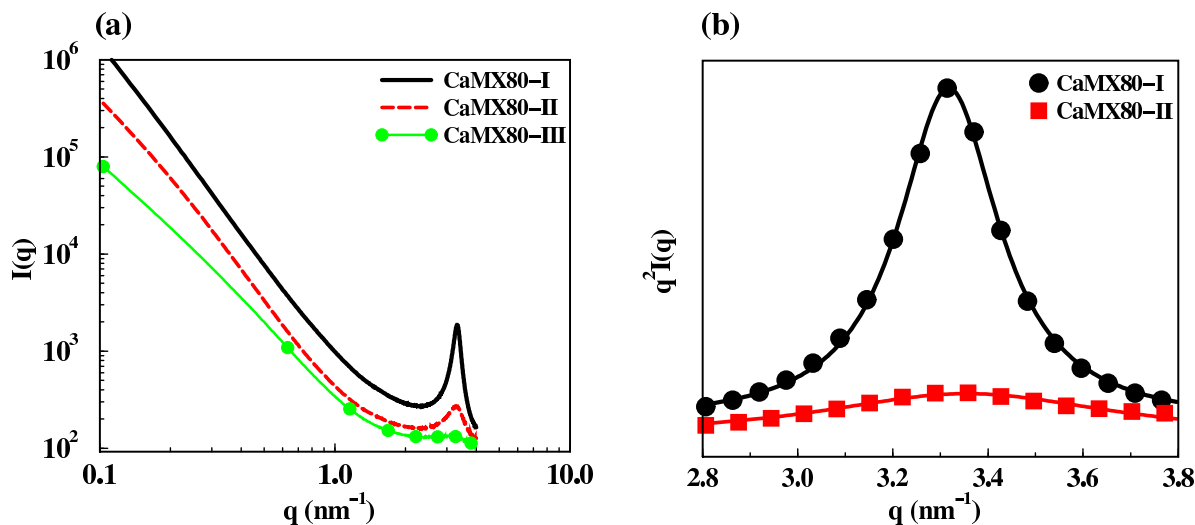


Fig. 4: (a) Scattering intensity as a function of wavevector for different CaMX80 fractions obtained from NaMX80 through equilibration with a 0.5 M  $\text{CaCl}_2$  solution. MX80-I is shown as black solid line, MX80-II red dashed line and MX80-III green solid line with symbols. (b) Fitting of the SAXS peak for MX80-I gives  $N \simeq 25$  (solid black line) and for MX80-II  $N \simeq 9$  (red dashed line). The peak for MX80-III is too broad to be analyzed. The solid lines are fits obtained from eq.(1) and symbols are measured values.

The number of platelets per aggregate,  $N$ , or the tactoid size can be estimated from the Scherrer formula.<sup>21</sup> Fig. 4 shows how the number of platelets in a tactoid varies with

platelet size. In this case, essentially all counterions are divalent calcium ions, which leads to a strong attraction between the charged platelets as a result of ion-ion correlations. The width of the SAXS peaks for the three fractions shows a significant difference. In particular the peak width of the sample with the smallest platelet size (CaMX80-III) displays a large broadening indicating that small aggregates of three platelets are present. As can be seen in Fig. 4b, the fitting procedure revealed that  $N \simeq 25$  and  $N \simeq 9$  for MX80-I and MX80-II, respectively. The effective diameter,  $D_{eff}$ , for the three fractions are about 950, 350 and 100 nm, respectively. This means that montmorillonite platelets smaller than 100 nm do not really form tactoids, in agreement with SAXS study.<sup>19</sup> Indeed, we have recently observed no tactoid formation in Laponite dispersions (results not shown here). Laponite is very small silicate nanoplatelets ( $\sim 30$  nm), the addition of enough salt reduces the electrostatic repulsion so that the platelets aggregate with a completely disordered microstructure. SAXS curves show a constant  $q$  position for all the peaks in the high- $q$  region, whereas a variation in the scattering intensities can be seen in the lower  $q$  value. The former observation indicates that the intra-lamellar distance is constant (1.9 nm) for all fractions of Ca montmorillonite (Fig. 4b), which is in agreement with predictions from MC simulations. As for the latter, one can notice a change in the slope from  $q^{-3.3}$  for thicker tactoids to  $q^{-2.3}$  for  $N \simeq 3$  (see Fig. 4a). We have previously reported that a dispersion of Na montmorillonite was already equilibrated with  $\text{Ca}^{2+}$  ions even at rather low bulk concentration (5mM  $\text{CaCl}_2$ ).<sup>18</sup> Thus, higher concentration of divalent salt in the bulk (0.5 M or more) appears to have little effect on the number of platelets per tactoid as well as on the exponent value in the low- $q$  regions. These results are in agreement with MC simulations.<sup>18,20</sup>

## Tactoid dissociation

In order to study tactoid dissociation a dispersion of fractionated clay (CaMX80-I) was placed in a dialysis pocket and immersed in a 2 L beaker of 50 mM NaCl solution and then allowed to equilibrate through exchange of ions at 298 K.

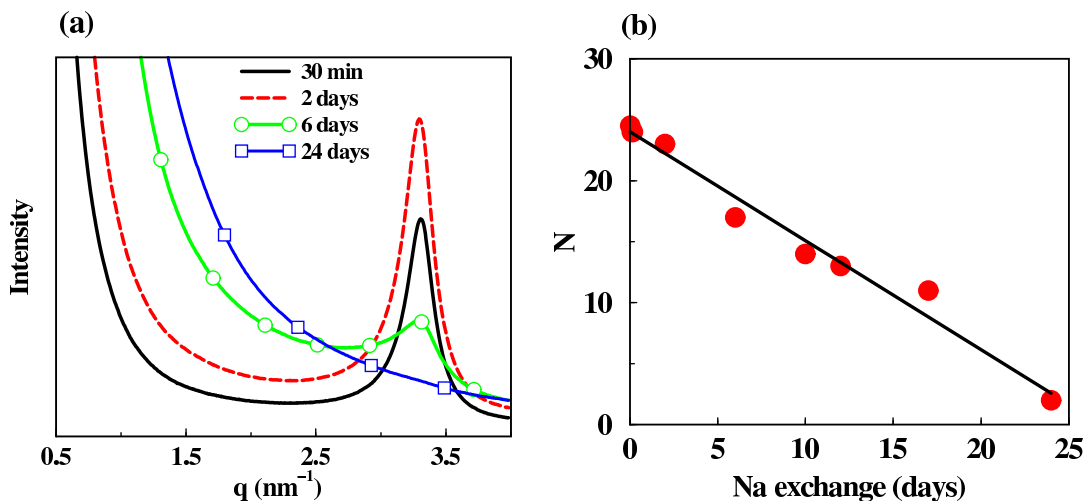


Fig. 5: (a) SAXS spectra from CaMX80-I dispersion equilibrated with a 50 mM NaCl solution for increasing time intervals from 30 min to 24 days as indicated in the graphs. (b) The number of platelets per tactoid,  $N$ , as a function of time for the system in (a).

As shown in Fig. 5a, SAXS spectra were collected at regular time intervals, where a Bragg peak arises from the well-ordered silicate layers in a tactoid. We observe a slow structural relaxation towards fully exfoliated platelets. Initially the peak intensity increases due to reduced sedimentation in the capillary cell targeted by X-rays, but the width increases as well, and the number of platelets per tactoid is a monotonically decreasing function of exchange time. After a week of Na exchange there are still tactoids present, but after three weeks the Bragg peak corresponding to a repeat distance of 1.9 nm has disappeared. In Fig. 5b, the number of platelets per tactoid as a function of Na exchange time was determined by fitting the SAXS data to the equation (1). The graph describes how the tactoids gradually dissociate when Ca montmorillonite is put in contact with a NaCl solution. Interestingly, the decay of  $N$  with time is approximately linear.

For an individual thin platelet the scattering intensity at low- $q$  follows a power law of the form  $I(q) = q^{-R}$ . The exponent value,  $R$ , for pure Na montmorillonite with randomly oriented platelets is  $\simeq 2$ .<sup>1,17,18</sup> The scattering intensity of CaMX80-I dispersion decays more rapidly than CaMX80-III with an approximate exponent of  $\simeq 3.3$ , see Fig. 4a. This indicates that  $R$  seems to be strongly affected by platelets size, as  $R \simeq 2.3$  for latter SAXS curve. Fig. 6 also shows that a high number of platelets per tactoid is related to a larger  $R$ . Here it

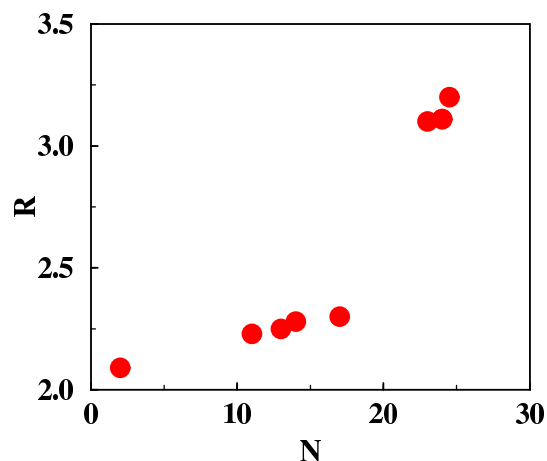


Fig. 6: The slope,  $R$ , of the scattering intensity at low- $q$  range as a function of tactoid size,  $N$ .

should be noted that adding different concentrations of NaCl only alter the kinetic reaction of the ion exchange from  $\text{Ca}^{2+}$  to  $\text{Na}^+$ . The values of  $R$  seem to change, as a consequence of the structural transition from aggregates to individual nanoplatelets or vice versa, see Fig. 4 and Fig. 5. Such values can be taken as an indication of the aggregate's length scale and how dense the microstructure is. In this context, the results in Fig. 3 demonstrate that each tactoid repels the nearest-neighbor tactoid, in agreement with the weak dependence between  $N$  and clay volume fraction found recently.<sup>19</sup> Scattering spectra, on the other hand indicate, platelet size controls the thickness of tactoids that form a large-scale structure, as for a specific tactoid size no change in  $R$  was observed over the low- $q$  ranges ( $q \simeq 0.01 - 1 \text{ nm}^{-1}$ ).<sup>31</sup> Thus, the systematic change in the scattering exponent describes the nano-to-mesoscale structure for silicate nanoplatelets.

### Tactoids from mixed size platelets

An interesting question is whether a clay dispersion composed of two size fractions of various ratios from the same or another mineral behaves differently from a single component system. To obtain a better understanding of tactoid formation in mixed nanoplatelet systems, we have used three different fractions of Na montmorillonite and kaolin platelets. NaBa-I is

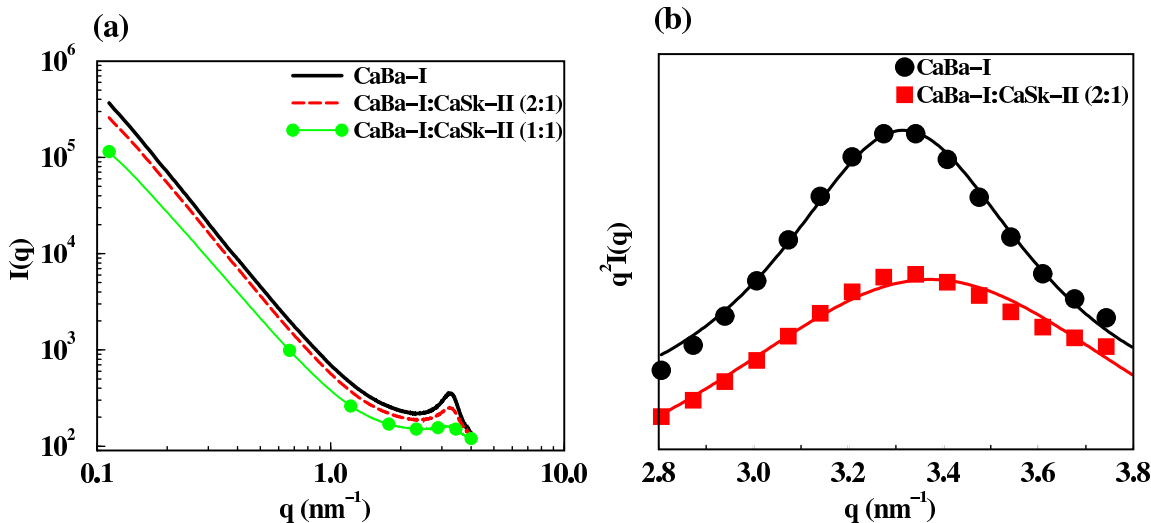


Fig. 7: (a) Scattering intensity as a function of wave vector for CaBa-I (solid line), and for CaBa-I and CaSk-II mixed in mass ratios of 2:1 (long dashed line) and 1:1 (green solid line with symbols). (b) The fitting procedure gives tactoid sizes of  $\approx 10$  and  $\approx 6$ . The dispersion with mass ratio 1:1 has a too broad peak to be analyzed. The solid lines are obtained from eq.(1).

composed of medium sized platelets ( $D_{eff} \simeq 350$  nm) similar to fraction II of NaMX80 and we know from earlier studies that with calcium counterions it forms tactoids. Platelets from fraction NaSk-II are much smaller ( $\sim 35$  nm) and pure CaSk-II does not form tactoids.

In a first set of SAXS experiments, a dispersion of either pure NaBa-I or a mixture of NaBa-I and NaSk-II with different weight ratios (2:1 and 1:1) were placed in separate dialysis pockets. These were allowed to equilibrate with 0.5 M  $\text{CaCl}_2$  at 298 K for a month exchanging  $\text{Na}^+$  counterions to  $\text{Ca}^{2+}$ . In Fig. 7a, one can observe the intra-lamellar distance in tactoids formed through the ion exchange of Bavarian and Slovakian montmorillonites. Indeed, peaks arise from the parallel arrangement of platelets at 1.9 nm in the tactoids. The platelet-platelet separation is the same as for other Ca clays, consistent with earlier SAXS data as well as MC simulations.<sup>6,11,13</sup> However, the tactoid size decreases with increasing amount of Slovakian montmorillonite. That is, addition of small platelets reduces the tactoid size. Thus, the required conditions for forming tactoids are divalent counterions and a sufficiently large platelets, in order to promote the correlation attraction between the negatively charged platelets.

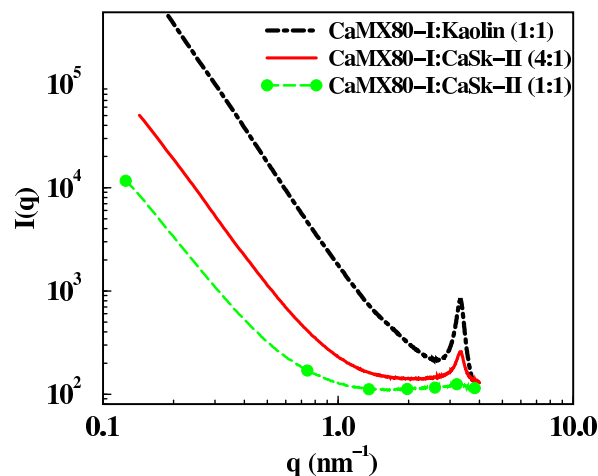


Fig. 8: (a) Scattering intensity  $I(q)$  as a function of wave vector for a mixture of CaMX80-I and kaolin, and for a mixture of CaMX80-I and CaSk-II with mass ratios (4:1) and (1:1) as indicated in graph.

In a second set of SAXS experiments we mixed NaMX80-I with NaSk-II in the same way as in the previous experiment in order to see the effect of a larger size ratio. The ratio between the effective diameter of NaBa-I and NaSk-II is about 10, while between NaMX80-I and NaSk-II it is almost 30, see Fig. 2 and Table 2. As can be seen in Fig. 8, adding small platelets of CaSk-II to CaMX80-I leads to an increase of peak width in the same way as in Fig. 7. The best fit to equation 2 for a single component of MX80-I ( $D_{eff} \simeq 950$  nm) gives  $N \simeq 25$ , whereas after mixing with CaSk-II the tactoid size decreases to  $\simeq 17$  (mass ratio 4:1) and with mass ratio 1:1 there is virtually no high  $q$  peak anymore. In Fig. 8, the scattering profile obtained for a 1:1 mixture of CaMX80-I and kaolin shows a sharp peak. The fitting procedure revealed that the tactoid size remains the same,  $N \simeq 25$ , as in pure CaMX80-I. Thus, there is no influence of the non-swelling kaolin clay on the intra-lamellar structure of Ca montmorillonite.

## Conclusions

We have investigated the tactoid formation and swelling behavior of montmorillonite platelets from three different sources, Wyoming, Bavaria and Slovakia, using small angle X-ray scattering and osmotic stress techniques. The platelet size distributions in natural montmoril-



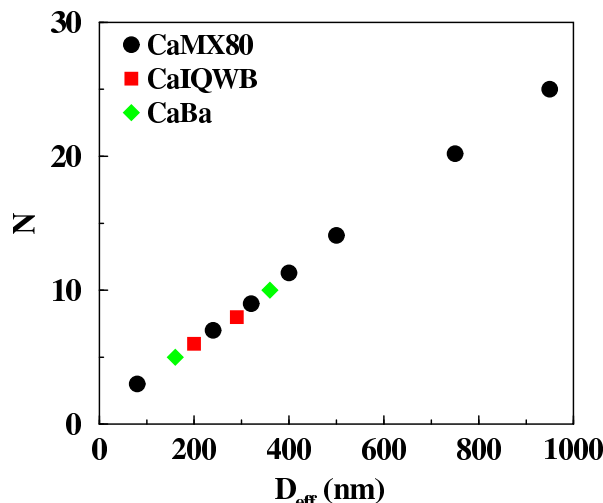


Fig. 9: Tactoid size,  $N$ , as a function of effective platelet size,  $D_{eff}$  for size fractionated clays of different natural origin.

lonites vary significantly and we have size-fractionated them. The platelet size in Slovakian and Bavarian montmorillonites is significantly smaller than that in the Wyoming montmorillonite. In the presence of divalent counterions the platelets aggregate into well ordered tactoids of limited size and with a well-defined spacing between the platelets. However, no tactoid formation was observed if the platelets are too small, *e.g.*  $\sim 30$  nm, as in the smallest fractions of Slovakian and Wyoming montmorillonites. The number of platelets per tactoid was determined from the scattering peak and the tactoid size scales linearly with the effective platelet size, see Fig. 9. We also found that the exponent value,  $R$ , is strongly affected by the aggregation number, which is in turn controlled by the platelets size. Mixing small non-tactoid forming platelets with larger platelets leads to a reduction of the tactoid size of the latter, while mixing with non-swelling clays, like kaolin, has no effect on tactoid formation. Montmorillonite platelets in equilibrium with seawater as well as most fresh water sources will have calcium as the dominating counterions. Under these circumstances, as the case for many nuclear waste repositories and storage technologies, tactoid formation will be crucial for the swelling behavior. By size-fractionating calcium montmorillonite, *e.g.* removing fractions with small platelets, one can reduce its swelling capacity as well as its hydraulic conductivity. This opens up interesting possibilities for tailoring of such properties.

## Acknowledgment

This study was financed by the Swedish Research Council through the Linnaeus grant Organizing Molecular Matter and supported by the Swedish Nuclear Fuel and Waste Management Company (SKB). M. Segad gratefully acknowledges the Royal Physiographic Society of Lund (KFS) for a number of grants including the Birgit and Hellmuth Hertz'. M. Segad also wants to express his appreciation to Z. Kaleh for joining the beamtime at MAXIV Laboratory. S. Kaufhold is thanked for kindly supplying the Bavarian and Slovakian clays. Bo Jönsson wants to express his appreciation for the interesting discussions with the personnel at ClayTech, Lund. This work is dedicated to Torbjörn Åkesson who passed away.

## References

- (1) L. J. Michot, I. Bihannic, F. Thomas, B. S. Lartiges, Y. Waldvogel, C. Caillet, J. Thieme, S. S. Funari and P. Levitz, *Langmuir*, 2013, **29**, 3500-3510.
- (2) A.V. Blackmore and B. P. Warkentin, *Nature*, 1960, **186**, 823-824.
- (3) I. Shomer and U. Mingelgrin, *Clays Clay Miner.*, 1978, **2**, 135-138.
- (4) L. L. Schramm and J. C. T. Kwak, *Clays Clay Miner.*, 1982, **30**, 40-48.
- (5) J. M. Cases, I. Berend, M. Francois, J. P. Uriot, L. J. Michot and F. Thomas, *Clays Clay Miner.*, 1997, **45**, 8-22.
- (6) A. V. Blackmore and R. D. Miller, *Soil Sci. Soc. Am. J.*, 1961, **25**, 169-173.
- (7) L. Guldbrand, Bo Jönsson, H. Wennerström and P. Linse, *J. Chem. Phys.*, 1984, **80**, 2221-2228.
- (8) R. J.-M. Pellenq, J. M. Caillol and A. Delville, *J. of Phys. Chem.*, 1997, **101**, 8584-8594.
- (9) R. Kjellander, S. Marčelja, and J. P. Quirk, *J. Coll. Interf. Sci.*, 1988, **126**, 194-211.

- (10) A. Thuresson, M. Ullner, T. Åkesson, C. Labbez and Bo Jönsson, *Langmuir*, 2013, **29**, 9216-9223.
- (11) K. Norrish, *Disc. Faraday Soc.*, 1954, **18**, 120-134.
- (12) M. Morvan, D. Espinat, J. Lambard, and Th. Zemb, *Colloids Surf.*, 1994, *82*, 193-203.
- (13) B. Jönsson, T. Åkesson, B. Jönsson, M. Segad, J. Janiak, and R. Wallenberg, *SKB Tech. Rep.*, 2009, *TR-09-06*, 1-34.
- (14) I. Shainberg, E. Bresler and Y. Klausner, *Soil Sci.*, 1971, **5**, 214-219.
- (15) D. Russo and E. Bresler, *Soil Sci. Soc. Am. J.*, 1977, **41**, 706-710.
- (16) C. Martin , F. Pignon , A. Magnin, M. Meireles, V. Lelièvre, P. Lindner and B. Cabane, *Langmuir*, 2006, **22**, 4065-4075.
- (17) M. Segad, S. Hanski, U. Olsson, J. Ruokolainen, T. Åkesson, Bo Jönsson, *J. Phys. Chem. C*, 2012, **116**, 7596-7601.
- (18) M. Segad, Bo Jönsson and B. Cabane, *J. Phys. Chem. C*, 2012, **116**, 25425-25433.
- (19) M. Segad, *J. Appl. Cryst.*, 2013, **46**, 1316-1322.
- (20) M. Segad, Bo Jönsson, T. Åkesson and B. Cabane, *Langmuir*, 2010, **26**, 5782-5790.
- (21) A. L. Patterson, *Phys. Rev.*, 1939, **56**, 978-982.
- (22) S. Kaufhold and R. Dohrmann, *J. Colloid Interface Sci.*, 2013, **390**, 225-233.
- (23) S. Kaufhold, and R. Dohrmann, *Appl. Clay Sci.*, 2008, **39**, 50-59.
- (24) M. Knaapila, C. Svensson, J. Barauskas, M. Zackrisson, S. S. Nielsen, K. N. Toft, B. J. Vestergaard, L. Arleth, U. Olsson, J. S. Pedersen and Y. A. Cerenius, *J. Synchrotron Radiat.*, 2009 , **16**, 498-504.

- (25) A. L. Labrador, Y. Cerenius, C. Svensson, K. Theodor, and T. S. Plivelic, *J. Phys. Conf. Ser.*, 2013, **425**, 072019.
- (26) A. P. Hammersley, S. O. Svensson, A. Thompson, H. Graafsma, E. Kvik and J. P. Moy, *Rev. Sci. Instr.*, 1995, **66**, 2729-2733.
- (27) H. J. Ploehn, and C. Y. Liu, *Rev. Sci. Instrum.*, 2006, **45**. 7025-7034.
- (28) H. Gao, S. Shori, X. Chen, H.-C. zur Loye and H. J. Ploehn, *J. Colloid Interface Sci.* **392**, 226-236 (2013).
- (29) I. D. Block and F. Scheffold *Rev. Sci. Instrum.*, 2010, **81**. 1231071-1231077.
- (30) L. Sun, J. T. Hirvi, T. Schatz, S. Kasa, and T. A. Pakkanen, *J. Phys. Chem. C*, 2015, ASAP.
- (31) M. Segad Meehdi, *Synchrotron X-ray Scattering and Monte Carlo Simulations of Structure and Forces in Silicate Nanoplatelet Dispersions*, Doctoral dissertation, Lund University, Lund, Sweden, 2014.

## TOC

